ORIGINAL ARTICLE

MOLECULAR DOCKING BASED IN-SILICO SCREENING OF PHYTOCHEMICALS FROM MEDICINAL PLANTS AS POTENTIAL ANTI-BACTERIAL AGENTS

Sabin Shrestha[1] ✉, **Abisa Ghimire[1]** ✉, **Sabita Raut[1]**, **Roshan Paudel[1]**, **Ayusha Shrestha[1]**,

Sushmita Bohora[1], **Bechan Raut[1]**, **Dharma Prasad Khanal[1]**

[1]*Department of Pharmacy, Manmohan Memorial Institute of Health Sciences, Soalteemode, Kathmandu, Nepal*

✉**Sabin Shrestha,**
Department of Pharmacy Manmohan Memorial Institute of Health Sciences, Soalteemode Kathmandu
Email: shresthasabin172@gmail.com

✉**Abisa Ghimire,**
Department of Pharmacy Manmohan Memorial Institute of Health Sciences, Soalteemode Kathmandu
Email: ghimireabisa@gmail.com

ABSTRACT

Introduction: The anti-bacterial resistance has risen in a hurry, and the scarcity of new anti-bacterial medications has become one of the foremost global issues in the 21st century. Antimicrobial resistance, specifically antibacterial resistance has emerged as an urgent global health issue that compromises the effectiveness of infection treatment and prevention. Antimicrobial resistance estimated in 2014 that by 2050, AMR might be the cause for 10 million deaths.

Method: In-silico method was utilized to investigate identify potential anti-bacterial medicinal plants. PyRx integrated version of AutoDock, open babble, vina wizard and Biovia discovery studio were utilized to predict the scoring functions of active chemical constituent from different medicinal plants, with specific protein of gram-positive and gram-negative bacteria. Discovery studio visualizer and marvin sketch was used to create 2D and 3D structure, interaction, and various web server was utilized to predict and collect the data.

Result: Thirty-one active chemical constituents of different medicinal plants were designed and docked with DNA gyrase of Escherichia coli PDB-ID [1KZN] and [5L3J], Penicillin binding protein of Staphylococcus aureus PDB-ID [3VSL] and [1VQQ]. Active chemical constituents of *Allium sativum* show very low binding affinity below -4.7 kcal/mol, Zanthoxylum armatum shows below -6.3 kcal/mol, *Zingiber officinale* shows moderate binding affinity below -6.9 kcal/mol, *Curcuma longa* shows highest binding affinity below -8.4 kcal/mol with DNA gyrase and Penicillin binding protein. Out of Thirty-one active chemical constituents A15 Curcumin (-7.2, -7.5, -7.7, -7.1 kcal/mol), A16 Demethoxycurcumin (-7.9, -7.5, -7.1, -7.6 kcal/mol) and A17 Bisdemethoxycurcumin (-8.2, -7.2 -6.9, -8.4) shows the highest binding affinity. Out of Thirty-one only two Active chemical constituents A16, A17 shows Lead likeness. Physiochemical, Lipinski's Rule and Pharmacokinetic parameters analyses shows that all active constituents have good physiochemical, pharmacokinetics parameters and moderate toxicological profile.

Conclusion: : In-silico analysis indicates a descending order of antibacterial potential *Curcuma longa > Zingiber officinale > Zanthoxylum armatum > Allium sativum,* based on molecular docking scores, physicochemical characteristics, Lipinski's Rule of Five, predicted pharmacokinetic parameters, and toxicological profile. Molecular docking results demonstrated that bioactive constituents of Curcuma longa, particularly curcuminoids and its derivatives (A15 - Curcumin, A16 - Demethoxycurcumin, A17 - Bisdemethoxycurcumin), exhibited the most favorable binding affinities toward selected bacterial target proteins, suggesting strong ligand receptor interactions and high inhibitory potential. Hence, Curcuma longa shows potential antibacterial action among four locally available medicinal plants.

Key words: **Molecular Docking, Anti-bacterial, DNA-Gyrase, *E-coli, Curcuma longa, Zingiber officinale, Zanthoxylum armatum, Allium sativum.***

INTRODUCTION

Microorganisms such as bacteria, fungi, parasites and viruses can evolve to the extent that and eventually become resistant to the antimicrobial drugs that are used to treat different diseases[1]. Since the rate of AMR has risen in a hurry, and the scarcity of new antimicrobial medications to tackle this problem, has become one of the foremost global issues in the 21st century. Antimicrobial resistance (AMR), specifically antibacterial resistance has emerged as an urgent global health issue that compromises the effectiveness of infection treatment and prevention[2-4]. Antimicrobial resistance (AMR) estimated in 2014 that by 2050, AMR might be the cause for 10 million deaths. A global assessment of the burden of bacterial AMR in 2019 was a recent step breakthrough in AMR epidemiology, revealing that, of the nearly 8.9 million deaths resulting from infections caused by bacteria that year, 1.27 million were related to AMR, and 4.95 million were linked to AMR[5-7].

Escherichia coli, Staphylococcus aureus, Klebsiella pneumoniae, Streptococcus pneumoniae, Acinetobacter baumannii, and P aeruginosa were the six main causes (73%) of AMR-associated mortality in 2019, reported to the 2022 Global Burden of Disease study[8]. Combating antimicrobial resistance (AMR) requires a comprehensive and integrated strategy including better prevention and control measure for infections, broadened global policies and funding, AMR surveillance systems, antimicrobial stewardship, upgraded knowledge about the mechanisms at the level of both individual and population, and the invention of novel antimicrobial treatment approaches[9].

Researchers figured out that plant-based antimicrobials have huge prospective to battle microbes with less side effects. Various parts of medicinal plants hold divergent medicinal properties against different microbes. Although numerous plant species have been tested for antibacterial- properties through several studies, potent plant species have not been sufficiently estimated[10]. The demand for plant-based drugs in the present generation is increasing promptly. It is a prerequisite to assess plants of medicinal value as they contain active constituents that aid consistently with various ailments used in traditional medicine for their promising biological activity[11].

An aromatic herbaceous annual spice, garlic (*Allium sativum L.*; Family: Amaryllidaceae). Organosulfur compounds, saponins, phenolic compounds, and polysaccharides represent some of the several bioactive substances found in garlic. Several studies have demonstrated the antioxidant, anti-inflammatory, antibacterial, antifungal, cardiovascular, anticancer, hepatoprotective, digestive system, anti-diabetic, anti-obesity, neuroprotective, digestive system, anti-diabetic, anti-obesity, neuroprotective, and renal protective curative effects of garlic. Garlic's antimicrobial properties are ascribed to its allicin activity, that has been observed to combat a broad range of microorganisms,

including bacteria that are resistant to antibiotics, including *Shigella, Enterococcus faecalis, Escherichia coli, Staphylococcus aureus, Proteus vulgaris, Pseudomonas aeruginosa, Vibrio, Streptococcus mutans, S. faecalis, S. pyogenes, Mycobacteria, Salmonella enterica,* and *Klebsiella aerogene* [12-14].

A perennial tuberous plant, turmeric (*Curcuma longa L.*) belonging to the family Zingiberaceae. Turmeric mostly consists of terpenoids, curcuminoids, and other phenolic compounds, Turmeric's antibacterial properties study have shown to inhibit the growth against a variety of gram-positive bacteria (*Staphylococcus aureus, Listeria innocua, and Enterococcus faecalis,*) and gram-negative bacteria (*Escherichia coli, Klebsiella pneumoniae and Pseudomonas sp.*)[15,16].

The sub deciduous fragrant shrub *Zanthoxylum armatum* is a member of the Rutaceae family. Leaves, fruits, stems, bark and seeds have shown to be composed of alkaloids, sterols, phenolics, lignins, coumarins, terpenoids, and flavonoids. Contributing particular significant in antioxidant, antimicrobial, antiviral, anti-inflammatory, hepatoprotective, cytotoxic, and insecticidal/larvicidal properties. Numerous gram-negative bacteria and gram-positive bacteria have been demonstrated to be hindered in their growth[17-19].

An aromatic, perennial herb, ginger (*Zingiber officinale Roscoe*), a member of the Zingiberaceae family. Phenolic compounds, terpenes, lipids, polysaccharides, organic acids, and raw fibers belong to its many chemical constituents. Multiple biological activities, such as anti-inflammatory, antioxidant, anticancer, antimicrobial, cardiovascular, neuroprotective, antidiabetic, antiobesity, antinausea, respiratory protective, and antiemetic properties[20].

Modern drug discovery increasingly relies on in-silico chemobiological approaches, which enhance the efficiency and accuracy of identifying potential therapeutic candidates. Among these methods, computer-aided drug design (CADD) plays a crucial role by integrating structural and biological information to support more rational and targeted drug development[21]. Molecular docking, a core technique within CADD, helps predict the binding interactions between ligands and biological targets, offering valuable structural insights into inhibitory mechanisms essential for lead optimization[22-24].

We hypothesize that active chemical constituents of the different medicinal plants showing anti-bacterial activity, locally available were designed through in-silico methods and docked with different specific target proteins to identify the most effective and potential antibacterial agents to combat antibiotic resistance.

METHODS

Ethics approval: The study protocol was approved by the Institutional Review Committee of Manmohan Memorial Institute of Health Sciences (MMIHS-IRC) NEHCO-IRC/081/064.

Procedure for selection of locally available medicinal plants as anti-bacterial.
The plants that have been used as anti-bacterial were identified and listed from various database like PubMed, Google Scholar, Research Gate etc. The selection of plants was carried out on the basis of availability of plant locally and biological activity[25-27].
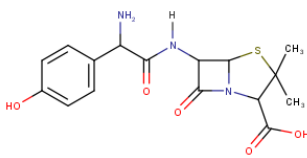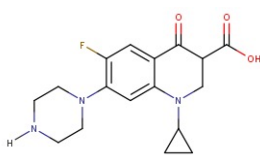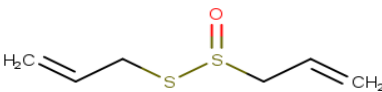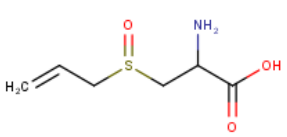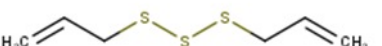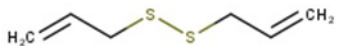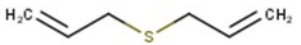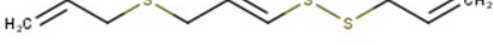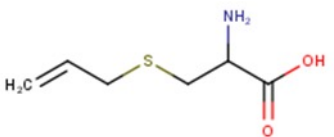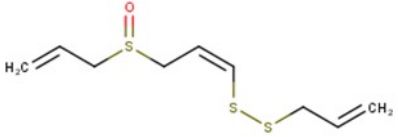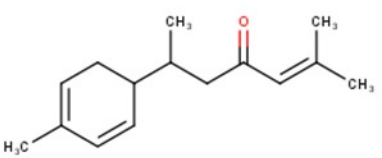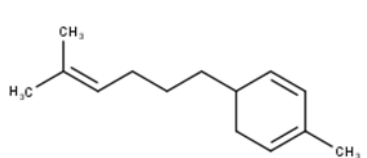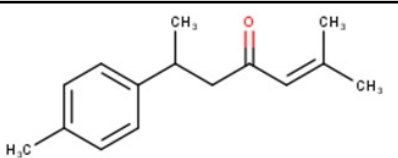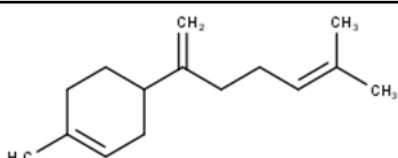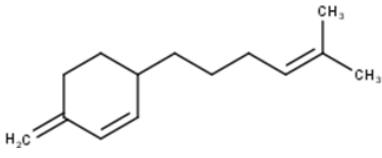
Molecular Docking software: PyRx integrated version of AutoDock, open babble, vina wizard and Biovia discovery studio were utilized to predict the scoring functions of active chemical constituent from di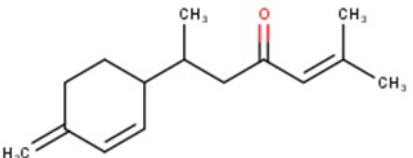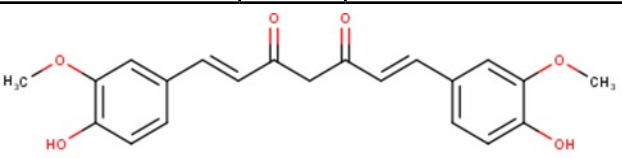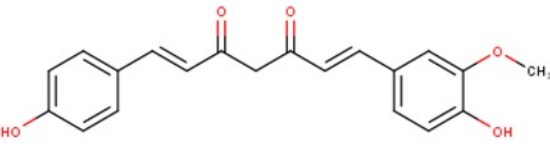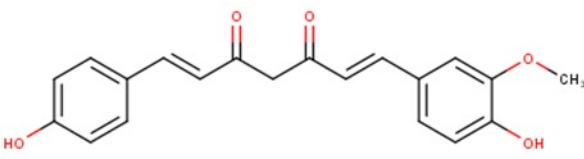fferent medicinal plants. Web-server https://www.swissadme.ch/, http://sts.bioe.uic.edu/, https://www.rcsb.org/, https://chatgpt.com/.[28] was utilized to predict physiochemical, pharmacokinetics, and taxological parameters

Preparation of 3D model of Ligand: Marvin Sketch: A sophisticated chemical editor, Marvin Sketch for drawing chemical structures, questions, and reactions. It is chemically aware and has a wide (and expanding) range of editing tools was employed to draw active chemical compounds in SDF format. These files were then converted into PDB and PDBQT format using Discovery Studio software. The ligands consisted of different range of phytochemical groups like Organosulfur compounds, alkaloids, saponins, terpenoids, flavonoids, phenolic compounds, glycosides and curcuminoids shown in Table – 1 and Figure - 1. [29]

Table 1: Active chemical constituents of different medicinal plants

Allium sativum		*Curcuma longa*	
Ligand	Name of Compound	Ligand	Name of Compound
A1	Allicin	A9	α-Turmerone
A2	Alliin	A10	α-Zingiberene
A3	Diallyl Trisulfide	A11	ar-Turmerone
A4	Diallyl Disulfide	A12	β-Bisabolene
A5	Diallyl Sulfide	A13	β-Sesquiphellandrene
A6	E-ajozene	A14	β-Turmerone
A7	S-Allyl-Cysteine	A15	Curcumin
A8	Z-ajozene	A16	Demethoxycurcumin
		A17	Bisdemethoxycurcumin
Zanthoxylum armatum		*Zingiber officinale*	
Ligand	Name of Compound	Ligand	Name of Compound
A18	E-methyl cinnamate	A22	α-Farnesene
A19	Limonene	A23	α-Zingiberene
A20	Linalool	A24	ar-curcumene
A21	Myrcene	A25	β-Bisabolene
		A26	β-Sesquiphellandrene
		A27	Gernial
		A28	Gingerol
		A29	Paradol
		A30	Shagaol
		A31	Zingerone

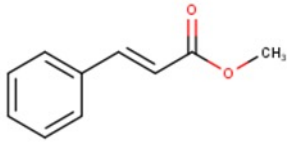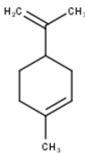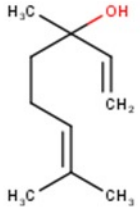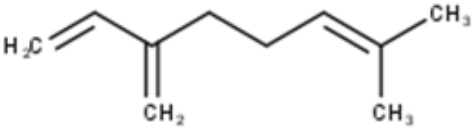| S.N.	STRUCTURE	S.N.	STRUCTURE
AMX		CIP	
A1		A2	
A3		A4	
A5		A6	
A7		A8	
A9		A10	
A11		A12	
A13		A14	
A15			
A16			
A17			
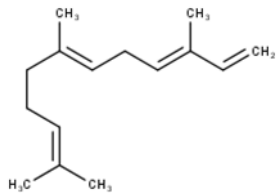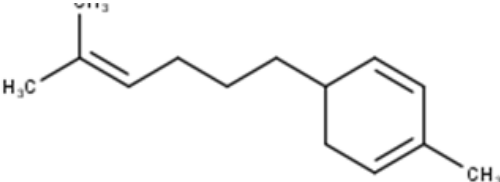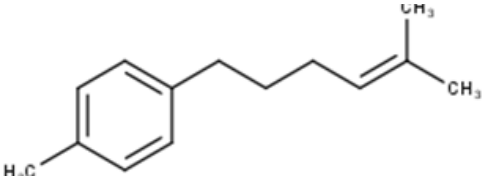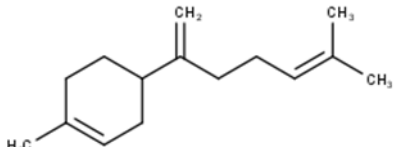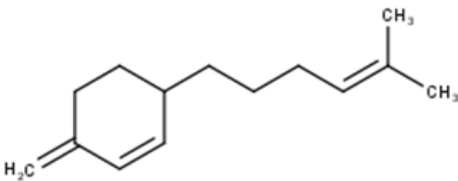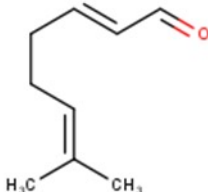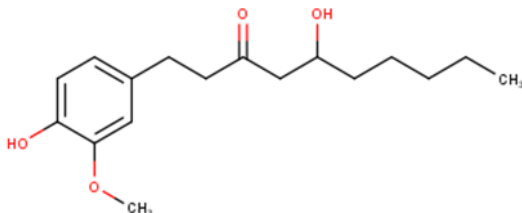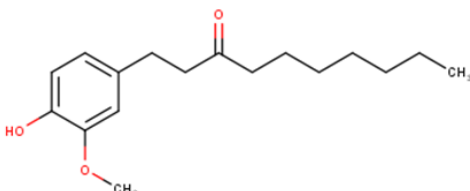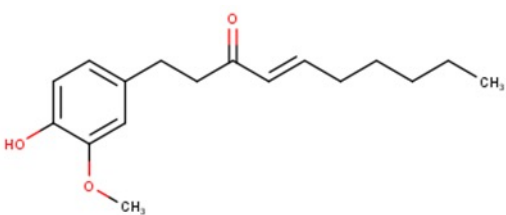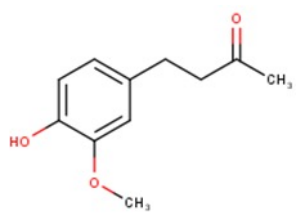
S.N.	STRUCTURE	S.N.	STRUCTURE
A18		A19	
A20		A21	
A22		A23	
A24		A25	
A26		A27	
A28		A29	
A30		A31	

Figure 1: 2D structure of Active chemical constituents of different medicinal plants.

Preparation and validation of target Protein: The target protein's X-ray crystal structures were obtained using the Protein Data Bank. The only global database for biological macromolecules structural data is Protein Data Bank (PDB; http://www.rcsb.org/pdb/) and screened on the basis of x-ray diffraction resolution, absence of mutations, and validation through the Ramachandran plot. Optimization involved cleaning the structure, removing irrelevant residues, correcting structural errors, and incorporating polar hydrogen bonds. The protein was validated by inbound ligand. The final refined structure was then saved in PDB format for further docking studies shown in Figure - 2[30].
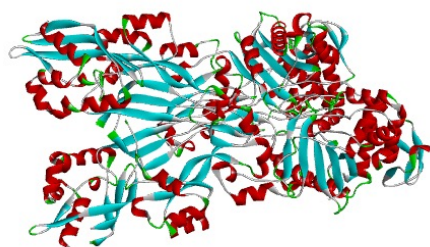
Crystal structure of the DNA gyrase of *Escherichia coli* [1KZN and 5L3J]	
PDB ID: [1KZN]	**PDB ID: [5L3J]**
Classification: Isomerase **Organism:** *Escherichia coli* **Expression system:** *Escherichia coli* **Mutation:** No **Method:** X-ray diffraction **Resolution:** 2.30Å	**Classification:** Isomerase **Organism:** *Escherichia coli* **Expression system:** *Escherichia coli* **Mutation:** No **Method:** X-ray diffraction **Resolution:** 2.83Å
Crystal structure of the PBP from *Staphylococcus aureus* [3VSL and 1VQQ]	
PDB ID: [3VSL]	**PDB ID: [1VQQ]**
Classification: Penicillin-binding Protein **Organism:** *Staphylococcus aureus* **Expression system:** *Escherichia coli* **Mutation:** No **Method**: X-ray diffraction **Resolution:** 2.40Å	**Classification:** Penicillin-binding Protein **Organism:** *Staphylococcus aureus* **Expression system:** *Escherichia coli* **Mutation:** No **Method:** X-ray diffraction **Resolution:** 1.80Å

Figure 2: 3D Crystal structure of the DNA gyrase and Penicillin-binding Protein

Identification of Binding Pocket: Computed Atlas of Surface Topography of proteins (CASTp) (http://cast.engr.uic.edu)[31] webserver was used to determine the active binding site of the target proteins. The active site was meticulously analysed and Active binding pockets of DNA gyrase [1KZN] have 12 active amino acid out of 205 amino acids and [5L3J] have 52 active amino acid out of 378 amino acids where as active binding site of Penicillin-binding Protein [3VSL] have 456 active amino acid out of 646 amino acids in chain A, B and [1VQQ] have 209 amino acid out of 646 amino acids in chain A, B shown in Figure – 3.

PDB ID: [1KZN]	**PDB ID: [5L3J]**
PDB ID: [3VSL]	**PDB ID: [1VQQ]**

Figure 3: Active binding pockets of target proteins.

Pharmacokinetic and Toxicity Prediction: The pharmacokinetic properties of all ligands, including gastrointestinal (GI) absorption, distribution, metabolism, and excretion (ADME), were predicted using the SWISS ADME web server (http://www.swissadme.ch/) [32]. Furthermore, their toxicity profiles were assessed using the ProTox-II web server (https://toxnew.charite.de/)[33], facilitating the identification of safe and effective drug candidates.

Biological Activity Prediction: To validate the docking results, the PASS web server (https://www.way2drug.com/passonline/) was utilized to predict the biological activity of the bioactive compounds, with 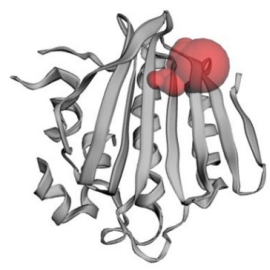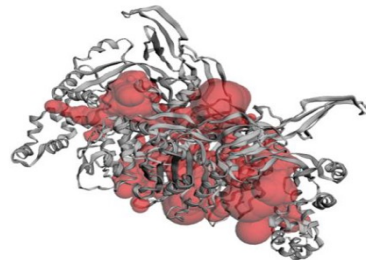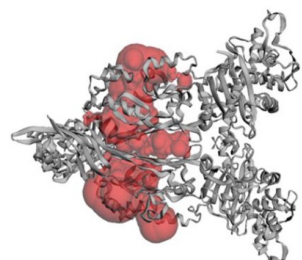a focus on antibacterial potential. The analysis revealed that the probability of activity (Pa) exceeded the probability of inactivity (Pi), indicating the compounds' potential antibacterial properties [34].

Docking Procedure:
Molecular docking was performed using AutoDock Vina to assess ligand–receptor interactions. The binding affinity was estimated using the equation: (3)

$$\Delta G_{Binding} = \Delta G_{Gauss} + \Delta G_{Repulsion} + \Delta G_{H\text{-}Bond} + \Delta G_{Hydrophobic} + \Delta G_{Tors}$$

Where:
$\Delta G_{Gaus} \rightarrow$ represents the dispersion of two Gaussian functions, $\Delta G_{Repulsion} \rightarrow$ accounts for repulsion beyond a threshold distance, $\Delta G_{H\text{-}Bond} \rightarrow$ models hydrogen bond interactions, $\Delta G_{Hydrophobic} \rightarrow$ is a ramp function for hydrophobic interactions, and $\Delta G_{Tors} \rightarrow$ is proportional to the number of rotatable bonds [3].

The protein structure was imported into AutoDock 4.2, converted to PDBQT format, and prepared for docking. Ligands were uploaded, their geometries were energy-minimized to obtain the most stable conformers, and then converted into PDBQT format for subsequent docking analysis. The docking grid parameters were set and obtained conformations were further analysed using Discovery Studio 2025.

RESULT AND DISCUSSION
Molecular docking analysis
Thirty-one active chemical constituents of different medicinal plants were designed and docked with DNA gyrase of *Escherichia coli* PDB-ID [1KZN] and [5L3J] to evaluate their potential antibacterial activity. The binding energy, number of hydrogen bonds, bond distance, and interacting amino acids are summarized in Table-2 and Figure-4. The ligand with the lowest binding energy, higher number of hydrogen bonds, shorter bond distance, and greater amino acid interactions was identified as the most promising candidate for further investigation.
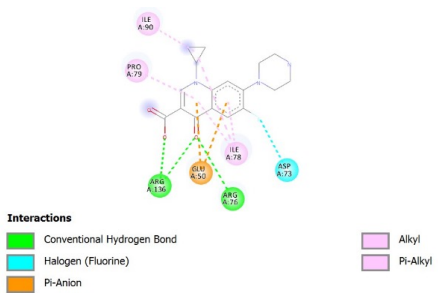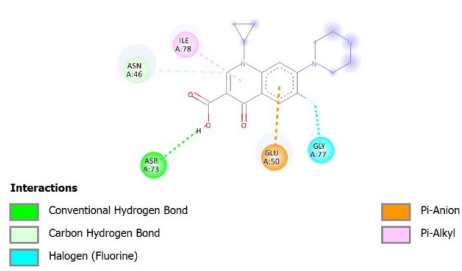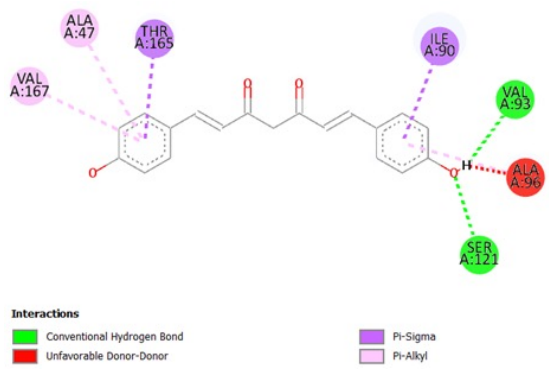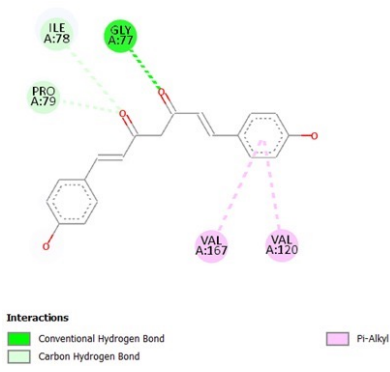
Binding affinity of the standard drug ciprofloxacin shows -7.6 kcal/mol, two hydrogen bonds, ARG -136, ARG -76, bond distance 2.72 and 2.88 Å with Protein [1KZN] and -6.3 kcal/mol. One hydrogen bond, ASP- 73, bond distance 2.64. most of the active chemical constituent of different plants shows low binding affinity as compare to standard drugs. *Allium sativum* show very low binding affinity below -4.7 kcal/mol with minimum number of hydrogen bond with [1KZN] and [5L3J], *Zanthoxylum armatum* shows low binding affinity below -6.3 kcal/mol with minimal number of hydrogen bond, *Zingiber officinale* shows moderate binding affinity below -6.9 kcal/mol with moderate number of hydrogen bond and *Curcuma longa* shows highest binding affinity below -8.2 kcal/mol and maximum number of hydrogen bond with both DNA-Gyrase [1KZN] and [5L3J]. Out of 31 ligands A15, A16, A17 active chemical constituents of *Curcuma longa* shows the best binding affinity and maximum number of hydrogen bond with DNA-Gyrase of *Escherichia coli* PDB-ID [1KZN] and [5L3J]. Hence, anti-bacterial properties of medicinal plants against DNA gyrase of *Escherichia coli* follow the order on the basis of binding affinity

Curcuma longa > Zingiber officinale > Zanthoxylum armatum > Allium sativum.

Table 2: Molecular docking result of active chemical constituents of *Allium sativum, Curcuma longa, Zanthoxylum armatum, Zingiber officinale* and standard Ciprofloxacin with DNA gyrase of *Escherichia coli.*

SN	Molecular docking result of *Allium sativum* with DNA gyrase of *Escherichia coli*					
	Protein [1KZN]			Protein [5L3J]		
	Binding energy (kcal/mol)	Number of H-bond	Amino acid with bond length	Binding energy (kcal/mol)	Number of H-bond	Amino acid with bond length
CIP	-7.6	2	ARG136:2.72, ARG76: 2.88	-6.3	1	ASP73:2.64
A1	-3.8	0	0	-3.8	1	THR165:2.86
A2	-4.6	2	VAL43:2.55, VAL71:2.17	-4.7	2	ASP73:1.97, THR165:2.75
A3	-3.7	0	0	-3.6	0	0
A4	-3.6	0	0	-3.6	0	0
A5	-3.6	0	0	-3.6	0	0
A6	-4.3	0	0	-4	0	0
A7	-4.3	3	GLY77:3.08, ASP73:2.95, THR165:2.84	-4.6	1	THR165:2.67
Molecular docking result of *Curcuma longa* with DNA gyrase of *Escherichia coli*						
	Protein [1KZN]			Protein [5L3J]		
A8	-4.3	1	0	-4	0	0
A9	-7.1	0	0	-6.6	0	0
A10	-6.4	0	0	-6.4	0	0
A11	-7.1	0	0	-6.7	0	0

A12	-6.9	0	0	-6.5	0	0
A13	-6.6	0	ASN46:2.23	-6.5	0	0
A14	-6.7	1	ASN46:2.23	-6.8	0	0
A15	-7.2	2	ASP73:2.61, SER121:2.16	-7.5	2	MET25:2.71, ARG190:2.67
A16	-7.9	2	VAL71:2.10, HIS95:2.18 VAL118:2.47	-7.5	4	LYS189:2.86, CYS268:2.10, GLY33:2.87, GLN275:2.56
A17	-8.2	2	VAL93:2.20, SER121:2.61	-7.2	1	GLY77:2.49
Molecular docking result of *Zanthoxylum armatum* with DNA gyrase of *Escherichia coli*						
	Protein [1KZN]			Protein [5L3J]		
A18	-5.8	1	GLY77:2.49	-6.3	1	GLY77:2.50
A19	-5.8	0	0	-5.9	0	0
A20	-5.6	1	VAL43:2.37	-4.9	1	GLU363:2.40
A21	-5.1	0	0	-5.4	0	0
Molecular docking result of *Zingiber officinale* with DNA gyrase of *Escherichia coli*						
	Protein [1KZN]			Protein [5L3J]		
A22	-6.1	0	0	-6.1	0	0
A23	-6.5	0	0	-6.4	0	0
A24	-6.6	0	0	-6.6	0	0
A25	-6.9	0	0	-6.5	0	0
A26	-6.6	0	0	-6.5	0	0
A27	-5.2	1	GLY77:2.29	-4.8	0	0
A28	-6.2	2	GLY77:2.89, ARG76:3.01	-5.9	0	0
A29	-6.2	1	GLY77:3.05	-5.8	0	0
A30	-6.6	2	ASN56:2.28, GLU50:2.31	-5.6	1	SER244:2.04
A31	-6.2	1	GLY71:3.07	-5.7	0	0

Standard with - [1KZN]	Standard with - [5L3J]
A17 with - [1KZN]	A17 with - [5L3J]

A16 with - [1KZN]	A16 with - [5L3J]

Figure 4: 2D interaction of CIP, A17 and A-16 with [1KZN] and [5L3J] protein.

Additionally, thirty-one active chemical constituents were docked with Penicillin binding protein of Staphylococcus aureus PDB-ID [3VSL] and [1VQQ] and are listed in Table 3 and Figure-5.
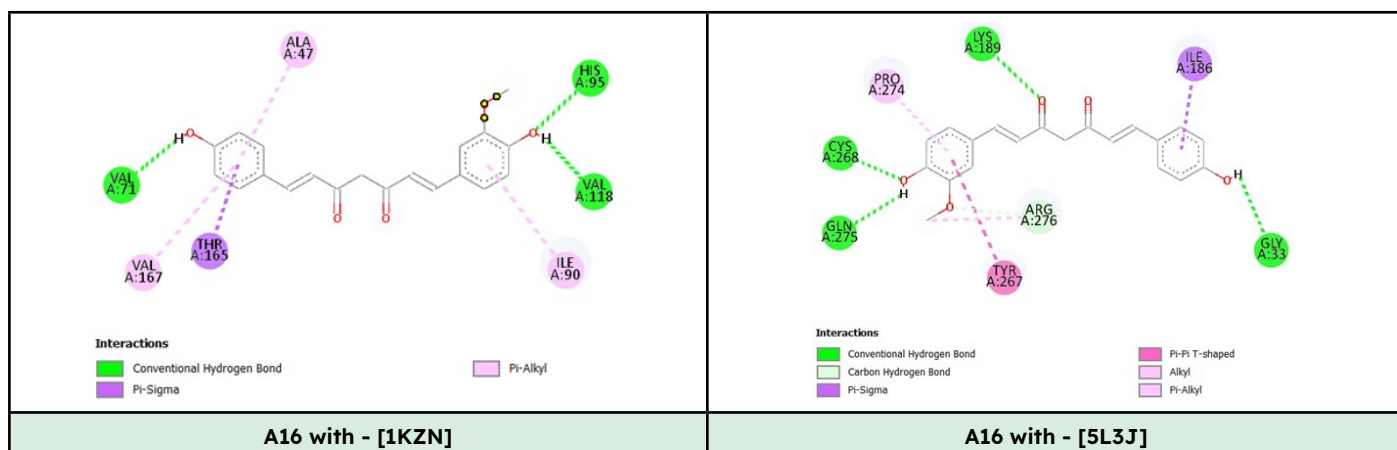
Binding affinity of the standard drug amoxicillin shows -8.3 kcal/mol, four hydrogen bonds, GLY-255, ARG-546, HIS-259, GLU-258 bond distance 3.28, 1.99, 2.23 and 2.64 Å with Protein [3VSL] and -7.5 kcal/mol, four hydrogen bonds, ARG-110, THR-312, HIS-311, ASN-111, bond distance 2.67, 2.45, 2.23 and 2.75. most of the active chemical constituents show low binding affinity as compare to standard drugs. *Allium sativum* show very low binding affinity below -4.7 kcal/mol with minimum number of hydrogen bond except A2 and A7, *Zanthoxylum armatum* shows low binding affinity below -6.1 kcal/mol with minimal number of hydrogen bond, *Zingiber officinale* shows moderate binding affinity below -6.1 kcal/mol with minimal number of hydrogen bond and *Curcuma longa* shows highest binding affinity below -7.7 kcal/mol and maximum number of hydrogen bond with Penicillin binding protein of *Staphylococcus aureus* PDB-ID [3VSL] and [1VQQ]. Out of 31 ligands A15, A16, A17 active chemical constituents of *Curcuma longa* shows the best binding affinity and maximum number of hydrogen bond with Penicillin binding protein of *Staphylococcus aureus* PDB-ID [3VSL] and [1VQQ]. Hence, anti-bacterial properties of medicinal plants against Penicillin binding protein of Staphylococcus aureus follow the order on the basis of binding affinity

Curcuma longa > Zingiber officinale > Zanthoxylum armatum > Allium sativum.

Table 3: Molecular docking result of active chemical constituents of *Allium sativum, Curcuma longa, Zanthoxylum armatum, Zingiber officinale* and standard amoxicillin with Penicillin binding protein of *Staphylococcus aureus*.

SN	Molecular docking result of *Allium sativum* with PBP of *S. aureus*					
	Protein [3VSL]			Protein [1VQQ]		
	Binding energy (kcal/mol)	Number of H-bond	Amino acid with bond length	Binding energy (kcal/mol)	Number of H-bond	Amino acid with bond length
AMX	-8.3	4	GLY255:3.28, ARG546:1.99, HIS259:2.23, GLU258:2.64	-7.5	4	ARG110:2.67, THR312:2.45, HIS311:2.23, ASN111:2.75
A1	-4.4	1	TYR636:2.58	-4.4	1	GLY282:1.93
A2	-4.7	4	THR621:2.83, SER392:2.26, SER448:2.83, THR603:2.84	-4.7	2	GLN113:2.52, GLY135:2.16
A3	-4.1	0	0	-4.1	0	0
A4	-3.4	0	0	-3.4	0	0
A5	-3.4	0	0	-3.4	1	TYR344:2.68
A6	-4.1	0	0	-4.1	1	LYS215:2.87
A7	-4.7	4	SER634:2.53, GLN656:2.05, TRP662:2.31, LEU663:1.92	-4.7	5	SER130:2.16, MET136:2.43, GLY135:2.42, ASP209:2.81,
Molecular docking result of *Curcuma longa* with PBP of *S. aureus*						
	Protein [3VSL]			Protein [1VQQ]		
A8	-4.3	2	ARG504:1.93,	-4.3	1	LYS318:2.00
A9	-6.7	1	ARG546:2.40	-6.3	1	ARG241:2.21, THR165:1.96
A10	-5.8	0	0	-5.6	0	0
A11	-6.5	0	0	-6.3	0	0

	Protein [3VSL]			Protein [1VQQ]		
A12	-6.5	0	0	-5.9	0	0
A13	-6.1	0	0	-5.8	0	0
A14	-6.8	0	ARG546:2.11	-6.3	2	ARG241:2.22, THR165:1.97
A15	-7.7	4	ASN450:2.13, LYS395:2.69, SER448:2.41, LEU663:2.75	-7.1	2	ARG65:2.49, ILE142:2.51
A16	-7.1	**2**	SER392:2.48, GLY620:2.37	-7.6	1	TYR196:3.08
A17	-6.9	1	ARG504:2.01	-8.4	2	GLU315:2.29, LYS318:2.43
Molecular docking result of *Zanthoxylum armatum* with PBP of *S. aureus*						
	Protein [3VSL]			**Protein [1VQQ]**		
A18	-5.8	0	0	-5.5	1	LYA68:2.55
A19	-6.1	0	0	-5.5	0	0
A20	-4.9	1	GLU255:2.61	-4.8	1	THR165:2.03
A21	-5.1	0	0	-4.4	0	0
Molecular docking result of *Zingiber officinale* with PBP of *S. aureus*						
	Protein [3VSL]			**Protein [1VQQ]**		
A22	-5.2	0	0	-5.3	0	0
A23	-6.1	0	0	-6	0	0
A24	-6.1	0	0	-5.6	0	0
A25	-6.1	0	0	-6.3	0	0
A26	-6.1	0	0	-6.1	0	0
A27	-5.1	0	0	-5	2	SER400:2.80, GLN521:2.05
A28	-5.2	0	0	-5.3	0	0
A29	-6.1	0	0	-6	0	0
A30	-6.1	0	0	-5.6	0	0
A31	-6.1	0	0	-6.3	0	0
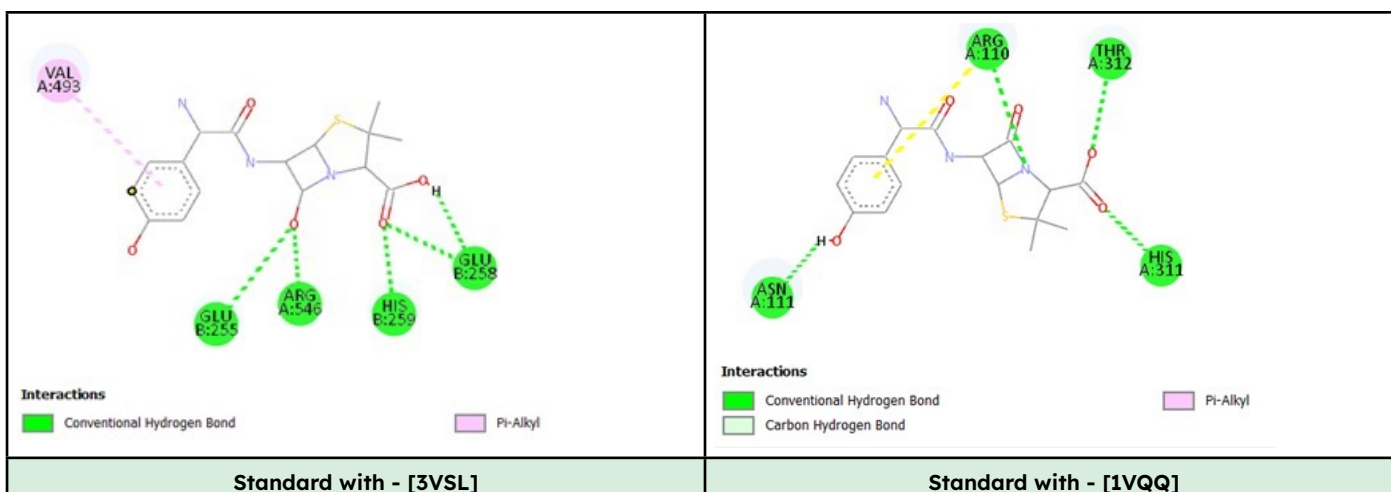
Standard with - [3VSL]	Standard with - [1VQQ]
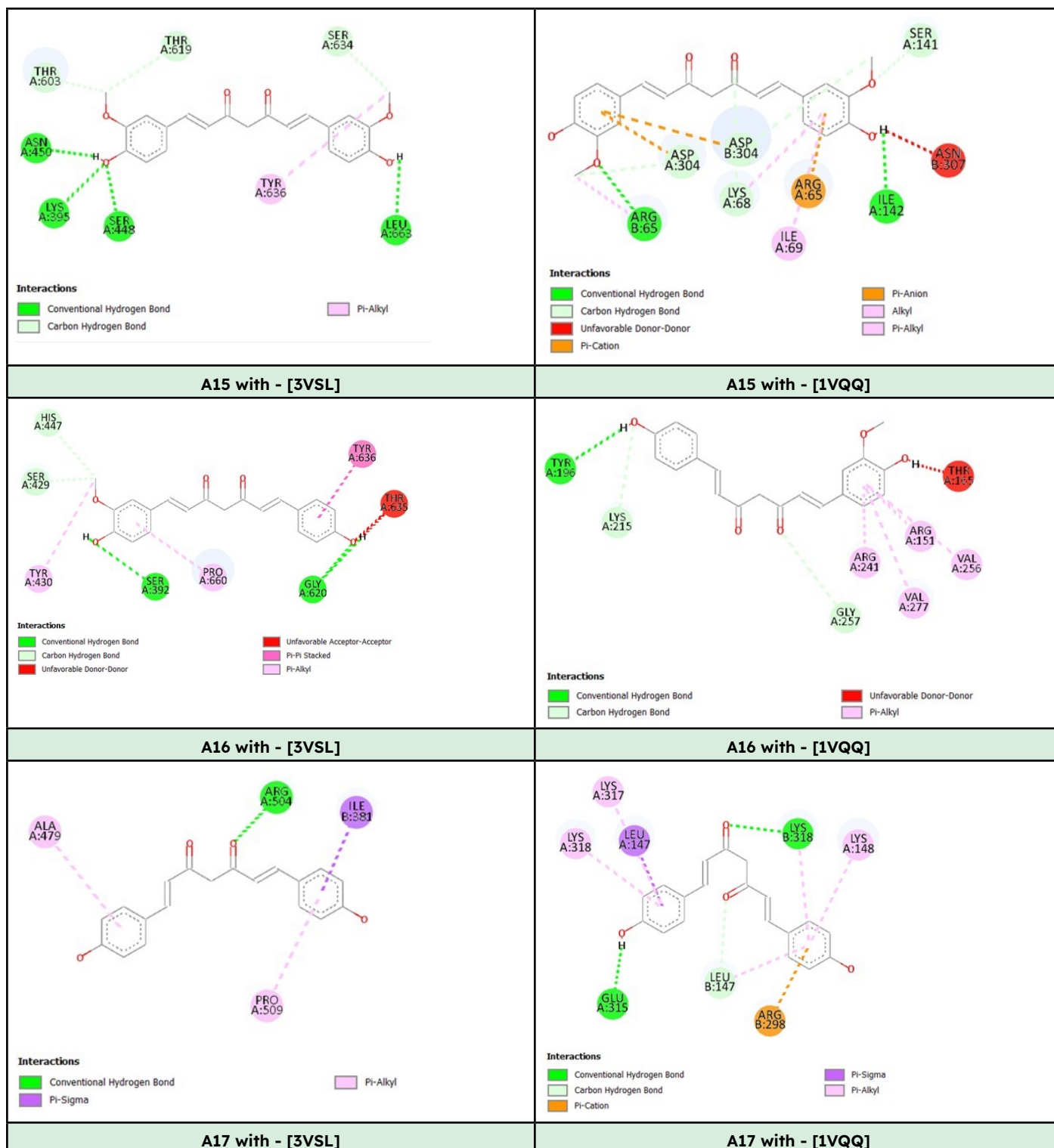
Figure 5: 2D interaction of AMX, A15, A16 and A-17 with [3VSL] and [1VQQ] protein.

Physiochemical, Lipinski's Rule and Pharmacokinetic parameters analyses: The molecular docking, binding affinity and scoring function was further validated by the drug's physicochemical properties and its absorption, distribution, metabolism, and excretion (ADME) characteristics, as presented in the Table-4. All derivatives comply with Lipinski's rule, exhibiting an optimal molecular weight of less than 500 Daltons, no more than 10 hydrogen bond acceptors, and no more than 5 hydrogen bond donors. Additionally, they demonstrate favourable lipophilic properties ranges from (0.5-4.6), most of the API have high GI-absorption except A1, A10, A12, A13, A19, A21-A26. Most of the API cross blood brain barrier. 20 out of 31 API shows interaction with CYP mostly 1A2, 3A4, 2C9, 2C19, 2D6. Lead likeness was shown by ciprofloxacin, A16 and A17. Physiochemical, Lipinski's Rule and Pharmacokinetic parameters analyses shows that all ligands have good ADME properties.

Table 4: Physiochemical, Lipinski's Rule and Pharmacokinetic parameters

SN	Mol Wt	RB	HA	HD	Log-p	Lip-Rule	GI-Abs	BBB	CYP-Inhibitors	Log-Kp	Lead Like
AMX	365	5	6	4	1.4	Yes	Low	No	No	-9.94	*No*
CIP	333	3	5	2	1.9	Yes	High	No	No	-8.53	*Yes*
A1	162	5	1	0	1.9	Yes	High	Yes	No	-6.36	No
A2	177	5	4	2	0.5	Yes	High	No	No	-9.89	No
A3	178	6	0	0	2.6	Yes	High	Yes	No	-5.51	No
A4	146	5	0	0	2.4	Yes	High	Yes	No	-5.63	No
A5	114	4	0	0	2.1	Yes	High	Yes	No	-5.46	No
A6	218	8	0	0	2.8	Yes	High	Yes	CYP2C1 CYP2C9	-5.50	No
A7	161	5	3	2	1.2	Yes	High	No	No	-8.75	No
A8	234	8	1	0	2.6	Yes	High	No	CYP2C9	-6.52	No
A9	218	4	1	0	3.1	Yes	High	Yes	CYP2C19 CYP2C9	-4.96	No
A10	190	4	0	0	3.5	Yes	Low	No	CYP2C9	-3.97	No
A11	216	4	1	0	3.1	Yes	High	Yes	No	-4.79	No
A12	204	4	0	0	4.6	Yes	Low	No	CYP2C9	-2.98	No
A13	190	4	0	0	4.3	Yes	Low	No	CYP2D9	-3.8-	No
A14	218	4	1	0	3.1	Yes	High	Yes	CYP2C19 CYP2C9	-4.78	No
A15	368	8	6	2	3.2	Yes	High	No	CYP2C9 CYP3A	-6.28	No
A16	338	7	5	2	2.7	Yes	High	No	CYP1A9 CYP2C9 CYP3A4	-6.01	Yes
A17	308	6	4	2	1.7	Yes	High	Yes	CYP1A9 CYP2C9 CYP3A4	-5.87	Yes
A18	162	3	2	0	2.3	Yes	High	Yes	No	-5.43	No
A19	136	1	0	0	2.7	Yes	Low	Yes	CYP2C9	-3.89	No
A20	154	4	1	1	2.7	Yes	High	No	No	-5.13	No
A21	136	4	0	0	2.8	Yes	Low	Yes	No	-4.17	No
A22	204	6	0	0	3.8	Yes	Low	No	CYP2C9	-3.20	No
A23	190	4	0	0	3.5	Yes	Low	No	CYP2C9	-3.97	No
A24	188	4	0	0	3.3	Yes	Low	Yes	CYP2D6	-3.86	No
A25	204	4	0	0	3.6	Yes	Low	No	CYP2C9	-2.98	No
A26	190	4	0	0	4.3	Yes	Low	No	CYP2D9	-3.80	No
A27	138	4	1	0	2.3	Yes	High	Yes	No	-5.43	No
A28	294	10	4	2	3.4	Yes	High	Yes	CYP1A2 CYP2D6	-6.14	No
A29	278	10	3	1	3.6	Yes	High	Yes	CYP1A2 CYP2D6	-5.08	No
A30	276	9	3	1	3.2	Yes	High	Yes	CYP1A2 CYP2C19 CYP2D6	-5.15	No
A31	194	4	3	1	2.0	Yes	High	Yes	CYP1A2	-6.70	No

Biological activity prediction: The biological activity prediction tool further endorses the docking parameters and pharmacokinetic parameters, and it displayed the antibacterial and antibiotic activity of 31 different ligands shown in Table - 5. All of the bioactive compounds had greater probability to be active (Pa) values than probability to be inactive (Pi) values. The findings revealed that all of these compounds have antibacterial as well as antibiotic activities.

Among 31 different ligands, A3, A13 and A26 showed highest biological activity whereas, A15 A16 and A17 exhibited moderate biological

activity prediction. The standards showed comparatively greater biological activity compared to the other ligands. probability of inactivity (Pi), suggesting that these compounds have potential antibacterial activity.

Table 5: probability of biological activity of highest [Pa] scoring API.

S.N.	Pa	Pi	Biological Activity
AMX	0,761 0,581	0,003 0,003	Antibacterial Antibiotic
CIP	0,551 0,321	0,012 0,012	Antibacterial Antibiotic
A3	0,486 0,152	0,018 0,048	Antibacterial Antibiotic
A13	0,474 0,239	0,019 0,021	Antibacterial Antibiotic
A15	0,272	0,071	Antibacterial
A16	0,270	0,072	Antibiotic
A17	0,325 0,101	0,051 0,081	Antibacterial Antibiotic

Toxicity Prediction: The toxicity assessment of thirty-one ligands was conducted to evaluate their safety profile. Various toxicological parameters, including hepatotoxicity (liver toxicity), neurotoxicity (nervous system toxicity), nephrotoxicity (kidney toxicity), cardiotoxicity (heart toxicity), cytotoxicity (cell toxicity), and immunotoxicity (immune system toxicity), were carefully examined. The toxicity of all 31 bio-active compounds of medicinal plants was predicted listed in Table - 6. Almost all prepared ligands lie in 4,5,6 classes which are less toxic but few lies in class 3 which are toxic if consumed. A2 (Class 6, LD50 = 8000 mg/kg) and A9 (Class 6, LD50 = 10000 mg/kg) ligands showed low toxicological profile compared to others ligands. A15, A16 and A17 ligands lie in class 4 and 5, LD50=2000mg/kg, exhibited nephrotoxicity, cytotoxicity and immuno toxicity. Standards comparatively showed greater toxicological profile compared to active chemical constitutions. The analysis revealed that active chemicals less taxological profile than that of standard drugs. Hence these findings indicate a promising therapeutic profile, supporting the potential use of these all-active chemical constituents in drug development as antibacterial action.

Table 6: Toxicity prediction of standard and active chemical constituents

S.N.	Class	LD50 Mg/kg	Hepato-Toxicity	Neuro-Toxicity	Nephro-Toxicity	Cyto-Toxicity	Cardio-Toxicity	Immune-Toxicity
AMX	4	1190	Active	Active	Inactive	Inactive	Inactive	Active
CIP	4	500	Inactive	Active	Active	Inactive	Inactive	Active
A2	6	8000	Inactive	Inactive	Inactive	Active	Inactive	Inactive
A9	6	10000	Inactive	Inactive	Inactive	Inactive	Inactive	Inactive
A15	4	2000	Inactive	Inactive	Active	Active	Inactive	Active
A16	4	2000	Inactive	Inactive	Active	Active	Inactive	Active
A17	5	2560	Inactive	Inactive	Active	Inactive	Inactive	Inactive

Note: LD50 values are given in [mg/kg]: Class I: fatal if swallowed (LD50 ≤ 5), Class II: fatal if swallowed (5 < LD50 ≤ 50), Class III: toxic if swallowed (50 < LD50 ≤ 300), Class IV: harmful if swallowed (300 < LD50 ≤ 2000), Class V: may be harmful if swallowed (2000 < LD50 ≤ 5000) and Class VI: non-toxic (LD50 > 5000).

CONCLUSION

Our in-silico analysis indicates a descending order of antibacterial potential as *Curcuma longa > Zingiber officinale > Zanthoxylum armatum > Allium sativum,* based on molecular docking scores, physicochemical characteristics, Lipinski's Rule of Five, predicted pharmacokinetic parameters, and toxicological profile. Molecular docking results demonstrated that bioactive constituents of Curcuma longa, particularly curcuminoids and its derivatives (A15 - Curcumin, A16 - Demethoxycurcumin, A17 - Bisdemethoxycurcumin), exhibited the most favourable binding affinities toward selected bacterial target proteins, suggesting strong ligand receptor interactions and high inhibitory potential. *Zingiber officinale* ranked second, with gingerols and related compounds showing stable docking conformations and competitive binding energies compared to curcuminoids. The antibacterial activity of *Zanthoxylum armatum* was moderate, with essential-oil constituents exhibiting reasonable binding affinities and physicochemical compatibility. *Allium sativum* showed the lowest overall ranking despite its well-known antimicrobial properties. This is largely due to the chemical instability and rapid metabolism

of its key bioactive compound, allicin, which adversely affects docking reliability and pharmacokinetic predictions. Although some garlic metabolites satisfy Lipinski's rule, their comparatively weaker binding affinities reduce their predicted antibacterial efficacy in silico. From a taxonomic perspective, members of the Zingiberaceae family (*Curcuma longa and Zingiber officinale*) demonstrated superior antibacterial potential. Overall, the combined molecular docking, physicochemical, and pharmacokinetic analyses support Curcuma longa as the most promising antibacterial candidate among four medicinal plants.

LIMITATIONS AND DIRECTIONS

This study presents several limitations that warrant consideration in future research. Firstly, only limited active chemical constituents were selected for in-silico investigation. Molecular docking and ADME analyses revealed promising candidate compounds, the lack of experimental validation such as in vitro or in vivo studies limits their potential for clinical application.

REFERENCES

1. Shen S, Qu X, Zhang W, Li J, Lv Z. Infection against infection : parasite antagonism against parasites , viruses and bacteria. Infect Dis Poverty. 2019;8(49):1–12.
2. Thapa RB. Antibiotic resistance patterns in uropathogens : insights from a Nepalese tertiary care setting. Ther Adv Infect Dis. 2025;12(1):1–7.
3. Shrestha S, Adhikari B, Thapa RB, Adhikari P. Exploring Aminopenicillin Resistance in Uropathogenic Staphylococcus species and Optimized Lead Prediction to Overcome Resistance through In- Silico Modules. J Nepal Chem Soc. 2025;45(2):45–63.
4. Shrestha S, Adhikari B, Thapa RB, Adhikari P, Bajracharya M, Giri U, et al. Exploring Aminopenicillin Resistance in Uropathogenic Escherichia Coli And Optimized Lead Prediction to Overcome Resistance Through New Generation Tools. J Manmohan Meml Inst Heal Sci. 2025;10(1):22–30.
5. Acar J, Rostel B. Antimicrobial resistance: an overview. Rev Sci Tech. 2001;20(3):797–810.
6. Wah K, Tang K, Millar BC, Moore JE. Antimicrobial Resistance (AMR). Br J Biomed Sci. 2023;80(June):1–11.
7. Collaborators AR. Articles Global burden of bacterial antimicrobial resistance 1990 – 2021 : a systematic analysis with forecasts to 2050. 2024;404(1):1199–226.
8. Liu G. Analysis of the Distribution and Antibiotic Resistance of Pathogens Causing Infections in Hospitals from 2017 to 2019. 2 Evidence-Based Complement Altern Med. 2022;1(1):1–17.
9. Ho CS, Wong CTH, Aung TT, Lakshminarayanan R, Mehta JS, Rauz S, et al. Review Antimicrobial resistance : a concise update. the Lancet Microbe2025. 2025;6(January):1–14.
10. Chandra H, Bishnoi P, Yadav A, Patni B, Mishra AP, Nautiyal AR. Antimicrobial Resistance and the Alternative Resources with Special Emphasis on Plant-Based Antimicrobials—A Review. mdpi. 2017;6(16):1–11.
11. Sumathi P, Parvathi A. Antimicrobial activity of some traditional medicinal plants. J Med Plants Res. 2010;4(4):316–21.
12. Batiha GE, Beshbishy AM, Wasef LG. Chemical Constituents and Pharmacological Activities of Garlic (Allium sativum L.): A Review. Nutrients. 2020;12(872):1–21.
13. Sasi M, Kumar S, Kumar M, Thapa S, Prajapati U, Tak Y, et al. Garlic (Allium sativum L .) Bioactives and Its Role in Alleviating Oral Pathologies. mdpi. 2021;10(1847):1–34.
14. L GA, Mavumengwana V, Li H. Bioactive Compounds and Biological Functions of Garlic (Allium sativum L.). mdpi. 2019;8(246):1–31.
15. Wu H, Liu Z, Zhang Y, Gao B, Li Y, He X. Chemical Composition of Turmeric (Curcuma longa L.) Ethanol Extract and Its Antimicrobial Activities and Free Radical Scavenging Capacities. mdpi. 2024;13(1550):1–13.
16. Chanda S, Ramachandra T V. Phytochemical and Pharmacological Importance of Turmeric (Curcuma longa): A Review. Res Rev A J Pharmacol. 2019;9(1):16–23.
17. Paul A, Kumar A, Singh G, Choudhary A. Medicinal , pharmaceutical and pharmacological properties of Zanthoxylum armatum : A Review. J Pharmacogn Phytochem 2018; 2018;7(4):892–900.
18. Phuyal N, Kumar P, Prasad P, Rajbhandary S. Zanthoxylum armatum DC .: Current knowledge , gaps and opportunities in Nepal. J Ethnopharmacol. 2018;8(10):1–16.
19. Singh SS. Antibacterial Activity of Zanthoxylum Armatum (Timur) on Gram Positive Bacteria and Gram Negative Bacteria. Res J Padmakanya Mult Campus. 2023;2(1):107–13.
20. Mao Q-Q, Xu X-Y, Cao S-Y. Bioactive Compounds and Bioactivities of Ginger (Zingiber o ffi cinale Roscoe). mdpi. 2019;8(185):1–21.
21. Gu R, Wu F, Huang Z. Role of Computer-Aided Drug Design in Drug Development. mdpi. 2023;28(7160):1–3.
22. Shrestha S, Khanal DP, Adhikari P, Thapa RB, Maji R. Molecular Docking Studies on The Anti-Cancer Activity of Novel Tri-Substituted Fluoro Indole Derivatives Against Human Topoisomerase-II Enzyme Using In- Silico Methods. J Manmohan Meml Inst Heal Scienes. 2024;9(1):35–42.
23. Shrestha S, Thapa RB. Molecular Docking Studies on the Anti-Cancer Activity of Novel Tri-Substituted Fluoro Indole Derivatives Against Human Topoisomerase-II Enzyme Using in-Silico Methods. J Manmohan Meml Inst Heal Scienes. 2024;9(1):35–42.
24. Shrestha S, Thapa RB, Adhikari P, Khanal DP. Exploring Resistance of Fluoroquinolones in Uropathogenic Escherichia coli and Optimized Lead Prediction Through In- Silico. Bull Pioneer Res Med Clin Sci. 2024;3(2):56–68.
25. White J. PubMed 2.0. Med Ref Serv Q. 2020;39(4):382–7.
26. acso P. As we may search – Comparison of major features of the Web of Science , Scopus , and Google Scholar citation-based and citation-enhanced databases. Curr Sci. 2005;89(9):1537–47.
27. Ovadia S. Behavioral & Social Sciences Librarian ResearchGate and Academia . edu : Academic Social Networks. Behav Soc Sci Librar. 2014;33(12):165–9.
28. Bikram R, Karki S, Shrestha S. Exploring potential drug-drug interactions in discharge prescriptions: ChatGPT's effectiveness in assessing those interactions. Explor Res Clin Soc Pharm. 2025;17(1):1–8.
29. Cherinka B, Andrews BH, Sánchez-Gallego J, Brownstein J, Argudo-Fernández M, Blanton M, et al. Marvin: A Tool Kit for Streamlined Access and Visualization of the SDSS-IV MaNGA Data Set. Astron J. 2019;158(2):1–15.
30. HM. Berman JW et al. The Protein Data Bank. Nucleic Acids Res. 2000;28(1):235–42.
31. Tian W, Chen C, Lei X, Zhao J, Liang J. CASTp 3.0: Computed atlas of surface topography of proteins. Nucleic Acids Res. 2018;46(W1):W363–7.
32. Daina A, Michielin O, Zoete V. SwissTargetPrediction: updated data and new features for efficient prediction of protein targets of small molecules. Nucleic Acids Res. 2019;47(W1):W357–64.
33. Banerjee P, Eckert AO, Schrey AK, Preissner R. ProTox-II: A webserver for the prediction of toxicity of chemicals. Nucleic Acids Res. 2018;46(W1):W257–63.
34. Filimonov DA, Lagunin AA, Gloriozova TA, Rudik A V., Druzhilovskii DS, Pogodin P V., et al. Prediction of the biological activity spectra of organic compounds using the pass online web resource. Chem Heterocycl Compd. 2014;50(3):444–57.

COMPETING INTERESTS

All the authors declare no competing interest

CRedit AUTHORSHIP CONTRIBUTION STATEMENT